Thermomagnetic renormalons in a scalar self-interacting $\lambda\phi^4$ theory

M. Loewe,[1,2,3] L. Monje,[1] and R. Zamora[4,5]

[1]*Instituto de Física, Pontificia Universidad Católica de Chile, Casilla 306, Santiago 22,Chile*
[2]*Centre for Theoretical and Mathematical Physics, and Department of Physics, University of Cape Town, Rondebosch 7700, South Africa*
[3]*Centro Científico-Tecnológico de Valparaíso CCTVAL, Universidad Técnica Federico Santa María, Casilla 110-V, Valparaíso, Chile*
[4]*Instituto de Ciencias Básicas, Universidad Diego Portales, Casilla 298-V, Santiago, Chile*
[5]*Centro de Investigación y Desarrollo en Ciencias Aeroespaciales (CIDCA), Fuerza Aérea de Chile, Casilla 8020744, Santiago, Chile*

(Received 7 May 2021; accepted 28 June 2021; published 20 July 2021)

In this article we extend a previous discussion about the influence of an external magnetic field on renormalons in a self-interacting scalar theory by including now temperature effects, in the imaginary formalism, together with an external weak external magnetic field. We show that the position of renormalons, which are poles in the Borel plane, does not change, getting their residues, however, a dependence on temperature and on the magnetic field. The effects of temperature and the magnetic field strength on the residues turn out to be opposite. We present a detailed discussion about the evolution of these residues, showing technical details involved in the calculation.

DOI: 10.1103/PhysRevD.104.016020

I. INTRODUCTION

Since the paper by Dyson [1] on the convergence of perturbative series in quantum electrodynamics (QED), a seminal article based exclusively on physical arguments, we have learned that power series expansions in quantum field theory, in general, are divergent objects. For high orders of perturbation, the divergence grows like $n!$, where n is the order of the expansion, and this is essentially due to the multiplicity of diagrams that contribute to a certain Green function, or to a physical process, at such an expansion order. A usual procedure to improve the convergence relies on the Borel transform [2–4]. However, in some cases, even the Borel-transformed series are divergent, spoiling the meaning of the whole procedure. The new singularities responsible for this divergent behavior are the renormalons. For a review, see Ref. [5]. Recently there has been a renewed interest in the subject by considering the one-loop renormalization group equation in multifield theories [6] or by considering a finite-temperature mass correction in the $\lambda\phi^4$ theory, reanalyzing the temperature dependence of poles and their residues [7]. There are other sources of divergences, such as instantons in quantum chromodynamics (QCD) [8,9]. However, we will not refer here to such objects that can be handled using semiclassical methods. In peripheral heavy-ion collisions, huge magnetic fields appear [10]. In fact, they are the biggest fields that exist in nature. The interaction between the produced pions in those collisions may be strongly affected by the magnetic field. Temperature is, of course, also present in such a scenario. In fact, several studies on the behavior of different physical parameters in the presence of an external magnetic field and/or temperature have been carried out by different authors. [11–33]. In this article we analyze, in the frame of a self-interacting scalar $\lambda\phi^4$ theory, the influence of the magnetic field and temperature on the position of the UV renormalons (the only ones relevant in $\lambda\phi^4$ theory) and their residues in the Borel plane. Recently, some extensions such as the q-Borel series have been proposed, allowing the discussion of series whose coefficients grow like $(k!)^q$ [34]. Also, there have been new attempts to find corrections to the beta function in QED with N_f flavors by considering closed chains of diagrams, like renormalons, and computing corrections of order N_f^{-2} and N_f^{-3} [35]. These authors found a new logarithmic branch cut whose physical role is not clear. The same situation will probably occur in self-interacting scalar theories with several components. In the present article we extend previous discussions where the behavior of renormalons in $\lambda\phi^4$ was analyzed, separately, for the case where thermal corrections appeared in the real time formalism, and for corrections due to the presence of a magnetic field. Here we present a discussion where both effects are simultaneously taken into account. As we will see, we need to handle the different possible scenarios with care. We discuss the high- and low-temperature cases for the weak magnetic field region, identifying the temperature- and magnetic-field-dependent subleading poles in the Borel plane. In the strong magnetic field regime there are no new singularities. A physical discussion will be presented. This article is organized as follows. In Sec. II we go through general aspects concerning a temperature- and magnetic-field-dependent scalar propagator. In Sec. III we present a brief discussion about the concept of Borel summable series and poles in the Borel plane. In Sec. IV we present the pure thermal discussion in the imaginary time formalism. Section V presents the general discussion, including temperature and magnetic field effects, about renormalon corrections to the propagator. Some technical details can be found in the Appendix. Finally, we present our conclusions.

II. THERMOMAGNETIC RENORMALON-TYPE CORRECTION TO THE PROPAGATOR

Thermomagnetic corrections will be handled through Schwinger's bosonic propagator at finite temperature. We are going to introduce the propagator by first taking only the external magnetic field into account, and then later incorporating finite-temperature effects. Schwinger's bosonic propagator is given by [36]

$$D^B(x', x'') = \phi(x', x'') \int \frac{d^4k}{(2\pi)^4} e^{-ik\cdot(x'-x'')} D^B(k), \quad (1)$$

where

$$iD^B(k) = \int_0^\infty \frac{ds}{\cos(eBs)} \times \exp\left(is\left[k_\parallel^2 - k_\perp^2 \frac{\tan(eBs)}{eBs} - m^2 + i\epsilon\right]\right). \quad (2)$$

The 4-momentum has been decomposed into parallel and perpendicular components with respect to the magnetic field direction. By considering a constant magnetic field, whose direction defines the z axis, we can write

$$(a\cdot b)_\parallel = a^0b^0 - a^3b^3, \qquad (a\cdot b)_\perp = a^1b^1 + a^2b^2 \quad (3)$$

for two arbitrary 4-vectors a_μ and b_μ. We also have

$$a^2 = a_\parallel^2 - a_\perp^2. \quad (4)$$

Notice that the phase factor in Eq. (1), given by

$$\phi(x', x'') = \exp\left(ie\int_{x''}^{x'} dx_\mu A^\mu(x)\right), \quad (5)$$

which is independent of the path, can be ignored for two-point functions which are diagonal in configuration space, as is the case in our analysis. As usual, we shall work in the momentum representation. In this way, using $eBs \to s$, we find

$$iD^B(k) = \frac{1}{eB}\int_0^\infty \frac{ds}{\cos(s)} \times \exp\left(i(s/eB)\left[k_\parallel^2 - k_\perp^2 \frac{\tan(s)}{s} - m^2 + i\epsilon\right]\right). \quad (6)$$

This propagator can be expressed as a sum over Landau levels [37],

$$iD^B(k) = 2i\sum_{l=0}^\infty \frac{(-1)^l L_l(\frac{2k_\perp^2}{eB}) e^{-k_\perp^2/eB}}{k_\parallel^2 - (2l+1)eB - m^2 + i\epsilon}, \quad (7)$$

where L_l are the Laguerre polynomials. By considering the previous expression in the region where $eB \ll m^2$, it is possible to show that [38]

$$iD^B(k) \xrightarrow{eB\to 0} \frac{i}{k_\parallel^2 - k_\perp^2 - m^2} - \frac{i(eB)^2}{(k_\parallel^2 - k_\perp^2 - m^2)^3} - \frac{2i(eB)^2 k_\perp^2}{(k_\parallel^2 - k_\perp^2 - m^2)^4}, \quad (8)$$

which is the desired weak-field expansion for our calculation. It is straightforward to generalize these expressions to the finite-temperature scenario through an analytic continuation into Matsubara frequency space [39,40], i.e.,

$$k_0 \to i\omega_n = \frac{2\pi n}{\beta}, \qquad n \in Z, \quad (9)$$

where $\beta = 1/T$, and where the integral in k_0 converts into a sum according to

$$\int \frac{d^4k}{(2\pi)^4} f(k) \to \frac{i}{\beta}\sum_{n\in Z}\int \frac{d^3k}{(2\pi)^3} f(i\omega_n, \vec{k}). \quad (10)$$

III. THE BOREL TRANSFORM

We will briefly present the Borel transform method, which can be considered as a tool designed to make sense of potentially divergent series [2]. For a divergent perturbative expansion

$$D[a] = \sum_{n=1}^\infty D_n a^n, \quad (11)$$

the Borel transform $B[b]$ of the series $D[a]$ is defined through

$$B[b] = \sum_{n=0}^{\infty} D_{n+1} \frac{b^n}{n!}. \qquad (12)$$

The inverse transform is

$$D[a] = \int_0^{\infty} db\, e^{-b/a} B[b]. \qquad (13)$$

We need the last integral to be convergent in order for the series to make sense, as $B[b]$ is free from singularities in the range of integration. If these conditions are fulfilled, we say that the original series $D[a]$ is Borel summable.

It is easy to check that all convergent series are also Borel summable. For divergent series this is not necessarily the case. If we find poles in the $0 - \infty$ range of integration of the previous equation, the series is no longer Borel summable. It is possible, however, to make sense of this integral in such cases through a prescription for the integration path in the complex $[b]$ plane, avoiding the pole. This will be, however, a prescription-dependent result.

A classical reference about divergent series is the book by Hardy [41].

It is known that perturbative expansions in quantum field theory are not Borel summable. There are two sources for the appearance of singularities in the Borel plane: renormalons and instantons. Here we do not want to comment about the latter possibility. In QCD, renormalons have been a matter of debate since these objects may affect our understanding of the gluon condensate [5].

IV. RENORMALONS IN THE VACUUM

In the $\lambda\phi^4$ theory the renormalon-type diagrams that produce poles in the Borel plane correspond to a correction to the two-point function.

First, we revise the calculation of this diagram with the insertion of k bubbles, then sum over k and study the behavior of its transform in the Borel plane.

We will denote by $R_k(p)$ the diagram of order k shown in Fig. 1, where p is the 4-momentum entering and leaving the diagram and q is the 4-momentum that goes around the chain of bubbles,

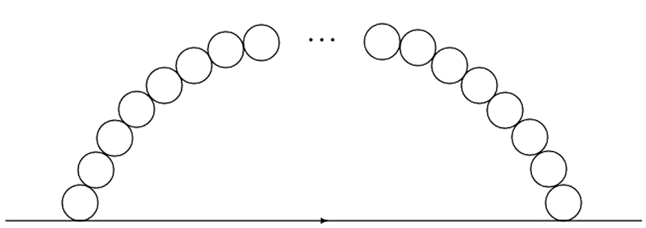

FIG. 1. Renormalon-type contribution to the two-point function.

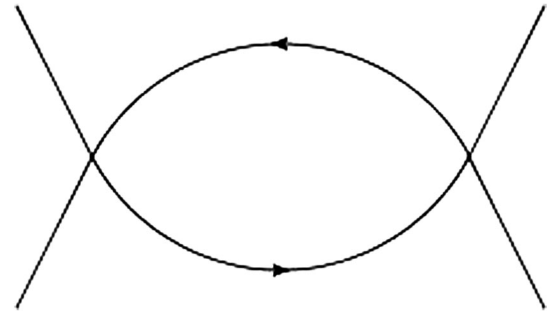

FIG. 2. Fish diagram.

$$R_k(p) = \int \frac{d^4q}{(2\pi)^4} \frac{i}{(p+q)^2 - m^2 + i\epsilon} \frac{[B(q)]^{k-1}}{(-i\lambda)^{k-2}}. \qquad (14)$$

In this expression, $B(q)$ corresponds to the contribution of one bubble in the chain, which is of course equivalent to the one-loop correction in the s-channel of the vertex, the so-called fish diagram (see Fig. 2). The factor $(-i\lambda)^{k-2}$ has been added to cancel the vertices that have been counted twice along the chain.

The expression for $B(q)$ is a well-known result [42],

$$B(q) = \frac{(-i\lambda)^2}{2} \int \frac{d^4k}{(2\pi)^4} \frac{i}{k^2 - m^2 + i\epsilon} \times \frac{i}{(k+q)^2 - m^2 + i\epsilon}, \qquad (15)$$

given by

$$B(q) = \frac{-i\lambda^2}{32\pi^2} \left[\Delta - \int_0^1 dx \log\left(\frac{m^2 - q^2 x(1-x) - i\epsilon}{\mu^2} \right) \right], \qquad (16)$$

where Δ is the divergent part that will be canceled by the counterterms, and μ is an arbitrary mass scale associated with the regularization procedure, which always appears when we go through the renormalization program.

The contribution to the renormalon comes from the deep Euclidean region in the integral in Eq. (14), i.e., where $-q^2 \gg m^2$. In this way, $B(q)$ in Eq. (16) can be approximated as

$$B(q) \approx \frac{-i\lambda^2}{32\pi^2} \log(-q^2/\mu^2). \qquad (17)$$

Inserting this result into Eq. (14) and performing a Wick rotation, we find

$$R_k(p) = \frac{-i\lambda^k}{(32\pi^2)^{k-1}} \int \frac{d^4q}{(2\pi)^4} \frac{1}{(p+q)^2 + m^2} \times [\log(q^2/\mu^2)]^{k-1}. \qquad (18)$$

This is an ultraviolet-divergent expression. However, since the theory is renormalizable, we can separate this expression into a finite and a divergent part. We are only interested in the finite part. For this, we expand the propagator in powers of $1/q^2$, neglecting the first two terms that leave divergent integrals, as we know this is justified due to the appearance of the counterterms.

So, we find

$$R_k = -i\left(\frac{\lambda}{32\pi^2}\right)^k 4m^4 \int_\Lambda^\infty dq[\log(q^2/\mu^2)]^{k-1} q^3 \times \left[\frac{m^4}{q^6} - \frac{m^6}{q^8} + \cdots\right], \tag{19}$$

with $\Lambda > 0$. The dependence on the external momentum p has disappeared. The lower limit Λ comes from the fact that we are interested in the deep Euclidean region. It has to be fixed in order to fulfill this condition.

Introducing $q = \mu e^t$ in the first two terms of Eq. (19) and fixing $\Lambda = \mu$, we find

$$\begin{aligned} R_k &= -i\left(\frac{\lambda}{32\pi^2}\right)^k \frac{4m^4}{\mu^2} \int_0^\infty dt e^{-2t}(2t)^{k-1} \times \left(1 - \frac{m^2}{\mu^2} e^{-2t}\right) \\ &= -i\left(\frac{\lambda}{32\pi^2}\right)^k \frac{2m^4}{\mu^2}\Gamma(k) + i\left(\frac{\lambda}{64\pi^2}\right)^k \frac{2m^6}{\mu^4}\Gamma(k) \\ &= -i\left(\frac{\lambda}{32\pi^2}\right)^k \tilde{m}^2\Gamma(k) + i\left(\frac{\lambda}{64\pi^2}\right)^k \frac{m^2}{\mu^2}\tilde{m}^2\Gamma(k), \end{aligned} \tag{20}$$

with $\tilde{m}^2 = 2m^4/\mu^2$. We see that this diagram grows like $k!$, thus inducing a pole in the Borel plane.

By taking the series ΣR_k,

$$D[\lambda] = \sum_k \frac{-i}{(32\pi^2)^k}\Gamma(k)\lambda^k, \tag{21}$$

its Borel transform is given by

$$\begin{aligned} B[b] &= \sum_k \left(\frac{R_k}{\lambda^k}\right)\frac{b^{k-1}}{(k-1)!}, \\ &= -i\tilde{m}^2 \frac{1}{1 - b/32\pi^2} + i\frac{m^2}{\mu^2}\tilde{m}^2 \frac{1}{1 - b/64\pi^2}, \end{aligned} \tag{22}$$

identifying, finally, the leading pole on the positive semireal axis in the Borel plane $b = 32\pi^2$ and the second pole in $b = 64\pi^2$.

V. THERMAL RENORMALONS

First we are going to calculate the renormalon contribution at finite temperature, and in the next section we will consider both temperature as well as the presence of a weak magnetic field. Although the finite-temperature calculation was considered in Ref. [43], that analysis was carried on in the frame of the real time formalism, more precisely thermo-field dynamics. We are now going to calculate the finite-temperature renormalon in the imaginary time formalism. There are some interesting technical details that are worth mentioning. The diagram to be calculated is

$$R_{T,k} = \frac{1}{(-i\lambda)^{k-2}} \int \frac{d^4q}{(2\pi)^4} iD(p+q)[B^T(q)]^{k-1}. \tag{23}$$

Notice that the $D(p+q)$ propagator could also be taken as temperature dependent. However, in our previous work [44] for the pure magnetic corrections case, we showed that if the propagator $D(p+q)$ included magnetic field contributions, taking also these magnetic corrections in the calculation of $B(q)$, subleading terms appear. Also, we showed that if we now take magnetic corrections for $D(p+q)$, as $B(q)$ is independent of the magnetic field, it has the same effect as taking $D(p+q)$ without a magnetic field and $B(q)$ with a magnetic field. The same situation also happens here when dealing with only temperature corrections. Therefore, our calculation will be carried out by considering $B(q)$ as temperature dependent, whereas $D(p+q)$ will be handled without temperature effects. First, let us consider one bubble,

$$B^T(q) = \frac{(-i\lambda)^2}{2} iT\sum_n \int \frac{d^3k}{(2\pi)^3} D^T(k)D^T(k-q), \tag{24}$$

where

$$D^T(k) = \frac{1}{\omega_n^2 + k^2 + m^2}, \tag{25}$$

and therefore

$$B^T(q) = \frac{(-i\lambda)^2}{2} iT\sum_n \int \frac{d^3k}{(2\pi)^3} \frac{1}{\omega_n^2 + k^2 + m^2} \times \frac{1}{(\omega_n - \omega)^2 + (k+q)^2 + m^2}. \tag{26}$$

The sum over Matsubara frequencies is calculated using well-known techniques [39] to obtain

$$B^T(q) = \frac{(-i\lambda)^2}{2} i \int \frac{d^3k}{(2\pi)^3} \frac{-s_1 s_2}{4E_1E_2} \times \frac{1 + n(s_1E_1) + n(s_2E_2)}{i\omega - s_1E_1 - s_2E_2}, \tag{27}$$

where

$$\begin{aligned} E_1^2 &= k^2 + m^2, \qquad s_1 = \pm 1, \\ E_2^2 &= (k+q)^2 + m^2, \quad s_2 = \pm 1, . \\ n_i(E_i) &= 1/(e^{E_i/T} - 1) \end{aligned}$$

Writing s_1 and s_2 explicitly, we obtain

$$\begin{aligned} B^T(q) = &\frac{(-i\lambda)^2}{2} i \int \frac{d^3k}{(2\pi)^3} \frac{1}{4E_1E_2} \\ &\times \left[(1+n_1+n_2) \left(\frac{1}{i\omega - E_1 - E_2} - \frac{1}{i\omega + E_1 + E_2} \right) \right. \\ &\left. - (n_1 - n_2) \left(\frac{1}{i\omega - E_1 + E_2} - \frac{1}{i\omega + E_1 - E_2} \right) \right] \\ &\equiv B_{\mathrm{vac}}(q) + B_T(q), \end{aligned} \tag{28}$$

where

$$\begin{aligned} B_{\mathrm{vac}}(q) = &\frac{(-i\lambda)^2}{2} i \int \frac{d^3k}{(2\pi)^3} \frac{1}{4E_1E_2} \\ &\times \left(\frac{1}{i\omega - E_1 - E_2} - \frac{1}{i\omega + E_1 + E_2} \right) \end{aligned} \tag{29}$$

is the vacuum part equal to Eq. (17) in the deep Euclidean region. Notice that we will use the notation $B^T(q)$ for the total fish diagram, including both vacuum and thermal corrections, whereas $B_T(q)$ will refer only to thermal corrections to the fish, where

$$\begin{aligned} B_T(q) = &\frac{(-i\lambda)^2}{2} i \int \frac{d^3k}{(2\pi)^3} \frac{1}{4E_1E_2} \\ &\times \left[(n_1+n_2) \left(\frac{1}{i\omega - E_1 - E_2} - \frac{1}{i\omega + E_1 + E_2} \right) \right. \\ &\left. - (n_1 - n_2) \left(\frac{1}{i\omega - E_1 + E_2} - \frac{1}{i\omega + E_1 - E_2} \right) \right] \end{aligned} \tag{30}$$

is the temperature-dependent part. Since the contribution to the renormalon comes from the deep Euclidean region, we calculate Eq. (30) in the limit $-q^2 \gg m^2$, obtaining

$$\begin{aligned} B_T(q) &\approx \frac{i\lambda^2}{4\pi^2 q^2} \int_0^\infty dk \frac{k^2}{\sqrt{k^2+m^2}} \frac{1}{e^{\sqrt{k^2+m^2}/T} - 1} \\ &\equiv \frac{i\lambda^2}{4\pi^2 q^2} h(\beta), \end{aligned} \tag{31}$$

with

$$h(\beta) = \int_0^\infty dk \frac{k^2}{\sqrt{k^2+m^2}} \frac{1}{e^{\sqrt{k^2+m^2}/T} - 1}. \tag{32}$$

Hence, the contribution for one bubble is

$$B^T(q) \approx \frac{-i\lambda^2}{32\pi^2} \left(\log(q^2/\mu^2) - \frac{8}{q^2} h(\beta) \right). \tag{33}$$

Now we have to insert this temperature-dependent fish diagram term into the chain of bubbles that define the renormalon-type diagram. We find

$$\begin{aligned} R_{T,k} = &\frac{1}{(-i\lambda)^{k-2}} \int \frac{d^4q}{(2\pi)^4} iD(p+q) \left(\frac{-i\lambda^2}{32\pi^2} \right)^{k-1} \\ &\times \left(\log(q^2/\mu^2) - \frac{8}{q^2} h(\beta) \right)^{k-1}. \end{aligned} \tag{34}$$

As we already mentioned, we proceed to expand the propagator $D(p+q)$ in powers of $1/q^2$, neglecting the first two terms that give rise to divergent integrals. We then have to calculate

$$\begin{aligned} R_{T,k} = &\frac{1}{(-i\lambda)^{k-2}} \int \frac{d^4q}{(2\pi)^4} \left[\frac{m^4}{q^6} - \frac{m^6}{q^8} + \cdots \right] \\ &\times \left(\frac{-i\lambda^2}{32\pi^2} \right)^{k-1} \left(\log(q^2/\mu^2) - \frac{8}{q^2} h(\beta) \right)^{k-1}. \end{aligned} \tag{35}$$

Using the binomial theorem

$$(A+B)^N = A^N + N \cdot A^{N-1} B + \cdots, \tag{36}$$

we get

$$\begin{aligned} R_{T,k} = &-i \frac{\lambda^k}{(32\pi^2)^{k-1}} \int \frac{d^4q}{(2\pi)^4} \left[\frac{m^4}{q^6} - \frac{m^6}{q^8} + \cdots \right] \\ &\times \left[\log(q^2/\mu^2)^{k-1} - (k-1) \frac{8}{q^2} h(\beta) \right. \\ &\left. \times \log(q^2/\mu^2)^{k-2} + \cdots \right]. \end{aligned} \tag{37}$$

Notice that the vacuum leading term as well as the next-to-leading-order vacuum term can be extracted from the first two terms inside the first square brackets, together with the first term of the second square brackets in the previous equation. The leading term in the magnetic field strength is obtained by multiplying the first term of the first square brackets with the second term of the second square brackets in the above equation. The next terms are subleading.

In this way, following the same procedure as in Sec. IV and performing the angular integrals, we find

$$R_{T,k} = -i4m^4\left(\frac{\lambda}{32\pi^2}\right)^k \int dq\left[\frac{(\log(q^2/\mu^2))^{k-1}}{q^3} - \frac{m^2}{q^5}\log(q^2/\mu^2)^{k-1} - \frac{(k-1)8h(\beta)(\log(q^2/\mu^2))^{k-2}}{q^5} + \cdots\right]. \quad (38)$$

Using the change of variable $q = \mu e^t$, $dq = \mu e^t dt$,

$$R_{T,k} = -i\left(\frac{\lambda}{32\pi^2}\right)^k \frac{4m^4}{\mu^2}\int dt\left[e^{-2t}(2t)^{k-1} - \frac{m^2}{\mu^2}e^{-4t}(2t)^{k-1} - \frac{(k-1)8h(\beta)e^{-4t}(2t)^{k-2}}{\mu^2} + \cdots\right], \quad (39)$$

we see the appearance of the gamma function in both terms. Using the definition of $\tilde{m}$, we have

$$R_{T,k} = -i\tilde{m}^2\left(\frac{\lambda}{32\pi^2}\right)^k \Gamma(k) + i\left(\frac{\lambda}{64\pi^2}\right)^k \frac{m^2}{\mu^2}\tilde{m}^2\Gamma(k) + 2i\frac{\tilde{m}^2}{\mu^2}\left(\frac{\lambda}{64\pi^2}\right)^k 8h(\beta)\Gamma(k) + \cdots, \quad (40)$$

where we have also used the property $\Gamma(z+1) = z\Gamma(z)$. Now we can find the Borel transform $B[b]$ of $\Sigma R_{T,k}$,

$$B[b] = \sum_k \left(\frac{R_{T,k}}{\lambda^k}\right)\frac{b^{k-1}}{(k-1)!}, = -i\tilde{m}^2\sum_k\left(\frac{1}{32\pi^2}\right)^k b^{k-1} + \left(\frac{im^2}{\mu^2}\tilde{m}^2 + \frac{i16h(\beta)\tilde{m}^2}{\mu^2}\right)\sum_k\left(\frac{1}{64\pi^2}\right)^k b^{k-1} + \cdots \quad (41)$$

These sums correspond to well-known geometrical series, and we obtain our final result

$$B[b] = \frac{-i\tilde{m}^2}{b - 32\pi^2} + \left(i\frac{m^2}{\mu^2}\tilde{m}^2 + \frac{i16h(\beta)\tilde{m}^2}{\mu^2}\right)\frac{1}{b - 64\pi^2} + \cdots \quad (42)$$

This result coincides with that reported in Ref. [43]. Although the location of the poles does not depend on temperature, the residues of these poles get a temperature dependence, and this behavior depends on the function $h(\beta)$. For details, see the Appendix.

VI. THERMOMAGNETIC RENORMALONS

In this section we calculate the renormalon contribution at finite temperature, also taking into account the presence of a weak external magnetic field. The expression for the diagram to be calculated now is given by

$$R_{B,T,k} = \frac{1}{(-i\lambda)^{k-2}}\int \frac{d^4q}{(2\pi)^4} iD(p+q)[B^{(T,B)}(q)]^{k-1}, \quad (43)$$

where (T, B) refers to finite-temperature and weak magnetic field effects. First, let us consider one bubble,

$$B^{(T,B)}(q) = \frac{(-i\lambda)^2}{2} iT\sum_n \int \frac{d^3k}{(2\pi)^3} i\tilde{D}^{(T,B)}(k) \times i\tilde{D}^{(T,B)}(k-q), \quad (44)$$

where $i\tilde{D}^{(T,B)}(k)$ is the finite-temperature propagator up to order $(eB)^2$ in the magnetic field, defined as

$$i\tilde{D}^{(T,B)}(k) \equiv iD^T(k) + iD^{(T,B)}(k), \quad (45)$$

with

$$iD^T(k) = -\frac{i}{\omega_n^2 + \vec{k}^2 + m^2}$$
$$iD^{(T,B)}(k) = \frac{i|eB|^2}{(\omega_n^2 + \vec{k}^2 + m^2)^3} - \frac{2i|eB|^2 k_\perp^2}{(\omega_n^2 + \vec{k}^2 + m^2)^4}. \quad (46)$$

Therefore, using this notation, Eq. (44) becomes

$$B^{(T,B)}(q) = \frac{(-i\lambda)^2}{2} iT\sum_n \int \frac{d^3k}{(2\pi)^3} \times (iD^T(k) + iD^{(T,B)}(k)) \times (iD^T(k-q) + iD^{(T,B)}(k-q)). \quad (47)$$

Note that the previous multiplication will produce terms of order greater than $(eB)^2$. If we restrict ourselves up to order $(eB)^2$, we obtain

$$B^{(T,B)}(q) = D_1(k,q) + D_2(k,q) + D_3(k,q), \quad (48)$$

with

$$D_1(k,q) = \frac{(-i\lambda)^2}{2} iT\sum_n \int \frac{d^3k}{(2\pi)^3} iD^T(k) iD^T(k-q), \quad (49)$$

$$D_2(k,q) = \frac{(-i\lambda)^2}{2} iT\sum_n \int \frac{d^3k}{(2\pi)^3} iD^T(k) iD^{(T,B)}(k-q), \quad (50)$$

$$D_3(k,q) = \frac{(-i\lambda)^2}{2} iT\sum_n \int \frac{d^3k}{(2\pi)^3} iD^{(T,B)}(k) iD^T(k-q). \quad (51)$$

It is straightforward to prove that $D_2(k,q) = D_3(k,q)$. Notice that $D_1(k,q)$ is the bubble with only temperature corrections obtained in the previous section [Eq. (24)], and hence

$$D_1(k,q) = \frac{-i\lambda^2}{32\pi^2}\left[\log\left(\frac{q^2}{\mu^2}\right) - \frac{8}{q^2}h(\beta)\right]. \tag{52}$$

Now we have to calculate $D_3(k,q)$. Since we know that $D_2(k,q) = D_3(k,q)$, we have

$$\begin{aligned} D_3(k,q) &= \frac{(-i\lambda)^2}{2} iT\sum_n \int \frac{d^3k}{(2\pi)^3} iD^{(T,B)}(k) iD^T(k-q) \\ &= \frac{(-i\lambda)^2}{2} iT\sum_n \int \frac{d^3k}{(2\pi)^3} \\ &\quad \times \left[\frac{i|eB|^2}{(\omega_n^2+\vec{k}^2+m^2)^3} - \frac{2i|eB|^2k_\perp^2}{(\omega_n^2+\vec{k}^2+m^2)^4}\right] \\ &\quad \times \left[-\frac{i}{(\omega_n-\omega)^2+(\vec{k}-\vec{q})^2+m^2}\right] \\ &\equiv D_{3.1}(k,q) + D_{3.2}(k,q), \end{aligned} \tag{53}$$

with

$$D_{3.1}(k,q) = \frac{(-i\lambda)^2 iT}{2}\sum_n \int \frac{d^3k}{(2\pi)^3}\frac{|eB|^2}{(\omega_n^2+\vec{k}^2+m^2)^3} \times \left[\frac{1}{(\omega_n-\omega)^2+(\vec{k}-\vec{q})^2+m^2}\right] \tag{54}$$

and

$$D_{3.2}(k,q) = \frac{(-i\lambda)^2 iT}{2}\sum_n \int \frac{d^3k}{(2\pi)^3}\frac{2|eB|^2k_\perp^2}{(\omega_n^2+\vec{k}^2+m^2)^4} \times \left[\frac{-1}{(\omega_n-\omega)^2+(\vec{k}-\vec{q})^2+m^2}\right]. \tag{55}$$

Let us first calculate $D_{3.1}(k,q)$,

$$D_{3.1}(k,q) = \frac{(-i\lambda)^2}{2\cdot 2!}\left(\frac{\partial}{\partial\tilde{m}^2}\right)^2 |eB|^2 iT\sum_n \int \frac{d^3k}{(2\pi)^3} \times \left[\frac{1}{\omega_n^2+\vec{k}^2+\tilde{m}^2}\right]\left[\frac{1}{(\omega_n-\omega)^2+(\vec{k}-\vec{q})^2+m^2}\right], \tag{56}$$

where we have used

$$\frac{1}{2!}\left(\frac{\partial}{\partial\tilde{m}^2}\right)^2 \frac{1}{k^2-\tilde{m}^2} = \frac{1}{(k^2-\tilde{m}^2)^3}. \tag{57}$$

Let us note that we again have the expression from the previous section [Eq. (26)], with the difference that we have to derive with respect to $\tilde{m}^2$ twice. In this way, we obtain

$$D_{3.1}(k,q) = \frac{|eB|^2(-i\lambda)^2 i}{2\cdot 2!} \times \left[\frac{2!}{32\pi^2m^2q^2} - \frac{1}{2\pi^2q^2}\left(\frac{\partial}{\partial\tilde{m}}\right)^2 h(\beta)\right]. \tag{58}$$

Note that the derivatives in $\tilde{m}$ have not been calculated because, as in the previous section, the function $h(\beta)$ needs to be analyzed separately for the low- and high-temperature cases. In a similar fashion, we calculate $D_{3.2}(k,q)$,

$$D_{3.2}(k,q) = \frac{(-i\lambda)^2}{3!}\left(\frac{\partial}{\partial\tilde{m}^2}\right)^3 |eB|^2 iT\sum_n \int \frac{d^3k}{(2\pi)^3} \times \left[\frac{k_\perp^2}{\omega_n^2+\vec{k}^2+\tilde{m}^2}\right] \times \left[\frac{-1}{(\omega_n-\omega)^2+(\vec{k}-\vec{q})^2+m^2}\right], \tag{59}$$

where we have used

$$\frac{1}{3!}\left(\frac{\partial}{\partial\tilde{m}^2}\right)^3 \frac{1}{k^2-\tilde{m}^2} = \frac{1}{(k^2-\tilde{m}^2)^4}. \tag{60}$$

Let us note that again we have the expression from the previous section [Eq. (26)], with the difference that we have to derive three times with respect to $\tilde{m}^2$. Hence, we obtain

$$D_{3.2}(k,q) = \frac{|eB|^2(-i\lambda)^2 i}{2\cdot 3!} \times \left[\frac{-3!}{96\pi^2m^2q^2} - \frac{2}{6\pi^2q^2}\left(\frac{\partial}{\partial\tilde{m}^2}\right)^3 k^2 h(\beta)\right]. \tag{61}$$

Taking into account the results $D_1(k,q)$, $D_2(k,q)$, and $D_3(k,q)$, we obtain for $B^{(T,B)}(q)$

$$\begin{aligned} B^{(T,B)}(q) = \frac{(i\lambda)^2}{2}\Bigg[&\frac{i}{16\pi^2}\log\left(\frac{-q^2}{\mu^2}\right) - \frac{8i}{16\pi^2q^2}h(\beta) \\ &+ 2|eB|^2 i\left\{\frac{1}{48\pi^2m^2q^2} - \frac{1}{2\pi^2q^2}\frac{1}{2!}\left(\frac{\partial}{\partial\tilde{m}^2}\right)^2 h(\beta)\right. \\ &\left. - \frac{1}{2\pi^2q^2}\frac{1}{3!}\left(\frac{\partial}{\partial\tilde{m}^2}\right)^3 h(\beta)\cdot k^2\right\}\Bigg]. \end{aligned} \tag{62}$$

As mentioned in the previous section, the function $h(\beta)$ cannot be calculated in a closed analytic form, but it can be expressed analytically for the cases of high and low temperature. Therefore, before calculating the renormalon diagram, we will calculate $B^{(T,B)}(q)$ for the cases of high and low temperature. In the high-temperature case, we calculate the corresponding derivatives using the expressions given in the Appendix to obtain

$$B_{\rm HT}(q) = -\frac{i\lambda^2}{32\pi^2}\left[\log\left(\frac{q^2}{\mu^2}\right) + \frac{1}{q^2}\left(-\frac{4\pi^2T^2}{3} + 2\pi mT - 2m^2\left(\frac{1}{2} + \log\left(\frac{4\pi T}{m}\right) - \gamma\right) - \frac{m^4}{T^2}\zeta(3) + \frac{m^6}{8\pi^4T^4}\zeta(5) + |eB|^2\left[\frac{7}{32m^2} - \frac{\pi T}{m^3} + \frac{1}{2\pi^2T^2}\zeta(3) - \frac{3m^2}{16\pi^4T^4}\zeta(5)\right]\right)\right]. \tag{63}$$

For the low-temperature case, we have

$$B_{\rm LT}(q) = -\frac{i\lambda^2}{32\pi^2}\left[\log\left(\frac{q^2}{\mu^2}\right) + \frac{1}{q^2}\left(-8\left(\frac{T^3m\pi}{2}\right)^{1/2}{\rm Li}_{3/2}(e^{-m/T}) + \frac{2|eB|^2}{3m^2} - 32|eB|^2\left[\frac{1}{32m^3}\left(\frac{\pi}{2mT}\right)^{1/2} \times [4m^2{\rm Li}_{-1/2}(e^{-m/T}) - 3T^2{\rm Li}_{3/2}(e^{-m/T})] + \frac{1}{384}\left(\frac{\pi}{2m^9T}\right)^{1/2}\left[3T\left(4m^2{\rm Li}_{1/2}(e^{-m/T}) + 5T\{2m{\rm Li}_{3/2}(e^{-m/T}) + T{\rm Li}_{5/2}(e^{-m/T})\}\right) - 8m^3{\rm Li}_{-1/2}(e^{-m/T})\right]\right]\right)\right]. \tag{64}$$

At this point, we have to calculate the renormalon-type diagram, both for high- and low-temperature regions, in the presence of a weak magnetic field.

A. Magnetic renormalons in the high-temperature region

Following the same procedure as in the previous section, we have to calculate the renormalon-type diagram

$$R^{\rm HT}_{B,T,k} = \frac{1}{(-i\lambda)^{k-2}}\int\frac{d^4q}{(2\pi)^4}iD(p+q)[B^{(T,B)}_{\rm HT}(q)]^{k-1}, \tag{65}$$

and we obtain

$$\begin{aligned}R^{\rm HT}_{B,T,k} &= -i\tilde{m}^2\left(\frac{\lambda}{32\pi^2}\right)^k\Gamma(k) + i\left(\frac{\lambda}{64\pi^2}\right)^k\frac{m^2}{\mu^2}\tilde{m}^2\Gamma(k)\\ &\quad - 2i\frac{\tilde{m}^2}{\mu^2}\left(\frac{\lambda}{64\pi^2}\right)^k\Gamma(k)\left(-\frac{4\pi^2T^2}{3} + 2\pi mT\right.\\ &\quad - 2m^2\left(\frac{1}{2} + \log\left(\frac{4\pi T}{m}\right) - \gamma\right) - \frac{m^4}{T^2}\zeta(3)\\ &\quad + \frac{m^6}{8\pi^4T^4}\zeta(5) + |eB|^2\left[\frac{7}{32m^2} - \frac{\pi T}{m^3}\right.\\ &\quad \left.\left.+ \frac{1}{2\pi^2T^2}\zeta(3) - \frac{3m^2}{16\pi^4T^4}\zeta(5)\right]\right) + \cdots\end{aligned} \tag{66}$$

This can be written as

$$\begin{aligned}R^{\rm HT}_{B,T,k} &\equiv -i\tilde{m}^2\left(\frac{\lambda}{32\pi^2}\right)^k\Gamma(k) + i\left(\frac{\lambda}{64\pi^2}\right)^k\frac{m^2}{\mu^2}\tilde{m}^2\Gamma(k)\\ &\quad - 2i\frac{\tilde{m}^2}{\mu^2}\left(\frac{\lambda}{64\pi^2}\right)^k\Gamma(k)F_{\rm HT} + \cdots,\end{aligned} \tag{67}$$

where

$$\begin{aligned}F_{\rm HT} &= -\frac{4\pi^2T^2}{3} + 2\pi mT\\ &\quad - 2m^2\left(\frac{1}{2} + \log\left(\frac{4\pi T}{m}\right) - \gamma\right) - \frac{m^4}{T^2}\zeta(3)\\ &\quad + \frac{m^6}{8\pi^4T^4}\zeta(5) + |eB|^2\left[\frac{7}{32m^2} - \frac{\pi T}{m^3}\right.\\ &\quad \left.+ \frac{1}{2\pi^2T^2}\zeta(3) - \frac{3m^2}{16\pi^4T^4}\zeta(5)\right].\end{aligned} \tag{68}$$

Now we can find the Borel transform $B[b]$,

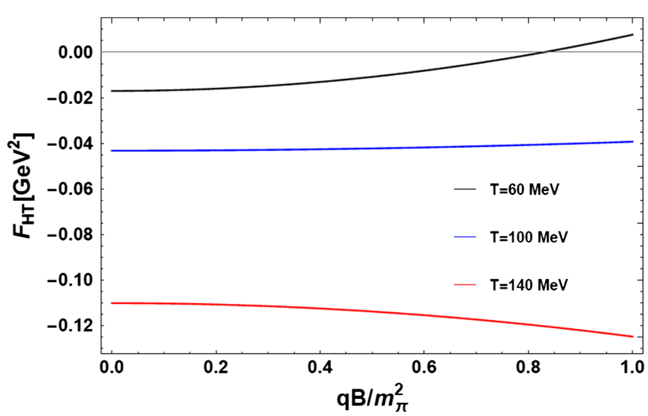

FIG. 3. $F_{\rm HT}$ vs T.

$$B[b] = \frac{-i\tilde{m}^2}{b-32\pi^2} + \left[i\frac{m^2}{\mu^2}\tilde{m}^2 - \frac{2i\tilde{m}^2}{\mu^2}F_{\mathrm{HT}}\right]\frac{1}{b-64\pi^2} + \cdots \tag{69}$$

As we mentioned, the location of the poles does not depend on temperature or the magnetic field. However, from Fig. 3 we notice a competition between temperature and the strength of the magnetic field for the evolution of the residue. For $T = 60$ MeV the curve grows with the magnetic field, but its concavity is low. When we start increasing the temperature, this concavity becomes smaller until we reach a temperature value where the sign of the concavity changes, implying this situation a decreasing behavior for the evolution of the residues of the renormalons. This indicates that temperature becomes dominant with respect to the magnetic field.

B. Magnetic renormalons in the low-temperature region

$$R^{\mathrm{LT}}_{B,T,k} = \frac{1}{(-i\lambda)^{k-2}}\int\frac{d^4q}{(2\pi)^4}\,iD(p+q)[B^{(T,B)}_{\mathrm{LT}}(q)]^{k-1}. \tag{70}$$

Again, we calculate in the same fashion as in the previous section. We obtain

$$\begin{aligned}R^{\mathrm{LT}}_{B,T,k} = &-i\tilde{m}^2\left(\frac{\lambda}{32\pi^2}\right)^k\Gamma(k) + i\left(\frac{\lambda}{64\pi^2}\right)^k\frac{m^2}{\mu^2}\tilde{m}^2\Gamma(k) - 2i\frac{\tilde{m}^2}{\mu^2}\left(\frac{\lambda}{64\pi^2}\right)^k\Gamma(k)\left(-8\left(\frac{T^3m\pi}{2}\right)^{1/2}\mathrm{Li}_{3/2}(e^{-m/T})\right.\\ &+\frac{2|eB|^2}{3m^2} - 32|eB|^2\left[\frac{1}{32m^3}\left(\frac{\pi}{2mT}\right)^{1/2}[4m^2\mathrm{Li}_{-1/2}(e^{-m/T}) - 3T^2\mathrm{Li}_{3/2}(e^{-m/T})]\right.\\ &+\frac{1}{384}\left(\frac{\pi}{2m^9T}\right)^{1/2}\left[3T\left(4m^2\mathrm{Li}_{1/2}(e^{-m/T}) + 5T\{2m\mathrm{Li}_{3/2}(e^{-m/T}) + T\mathrm{Li}_{5/2}(e^{-m/T})\}\right)\right.\\ &\left.\left.\left.-8m^3\mathrm{Li}_{-1/2}(e^{-m/T})\right]\right]\right) + \cdots\end{aligned} \tag{71}$$

It is convenient to write this (as we did in the high-temperature case) as

$$R^{\mathrm{LT}}_{B,T,k} \equiv -i\tilde{m}^2\left(\frac{\lambda}{32\pi^2}\right)^k\Gamma(k) + i\left(\frac{\lambda}{64\pi^2}\right)^k\frac{m^2}{\mu^2}\tilde{m}^2\Gamma(k) - 2i\frac{\tilde{m}^2}{\mu^2}\left(\frac{\lambda}{64\pi^2}\right)^k\Gamma(k)F_{\mathrm{LT}} + \cdots, \tag{72}$$

where

$$\begin{aligned}F_{\mathrm{LT}} = &-8\left(\frac{T^3m\pi}{2}\right)^{1/2}\mathrm{Li}_{3/2}(e^{-m/T}) + \frac{2|eB|^2}{3m^2} - 32|eB|^2\left[\frac{1}{32m^3}\left(\frac{\pi}{2mT}\right)^{1/2}[4m^2\mathrm{Li}_{-1/2}(e^{-m/T}) - 3T^2\mathrm{Li}_{3/2}(e^{-m/T})]\right.\\ &\left.+\frac{1}{384}\left(\frac{\pi}{2m^9T}\right)^{1/2}\left[3T\left(4m^2\mathrm{Li}_{1/2}(e^{-m/T}) + 5T\{2m\mathrm{Li}_{3/2}(e^{-m/T}) + T\mathrm{Li}_{5/2}(e^{-m/T})\}\right) - 8m^3\mathrm{Li}_{-1/2}(e^{-m/T})\right]\right].\end{aligned} \tag{73}$$

Now we can find the Borel transform $B[b]$,

$$B[b] = \frac{-i\tilde{m}^2}{b-32\pi^2} + \left[i\frac{m^2}{\mu^2}\tilde{m}^2 - \frac{2i\tilde{m}^2}{\mu^2}F_{\mathrm{LT}}\right]\frac{1}{b-64\pi^2} + \cdots \tag{74}$$

Again, we see that for low temperature and weak magnetic field, the location of the renormalons does not depend on temperature or the magnetic field. As we can see in Fig. 4, in the low-temperature region we have a growing evolution of the residue with the magnetic field. The curvature is bigger than that in the high-temperature region. This is reasonable since we are in the low-temperature region where the magnetic field dominates, although we already notice that for higher values of temperature the tendency of the residue is to diminish.

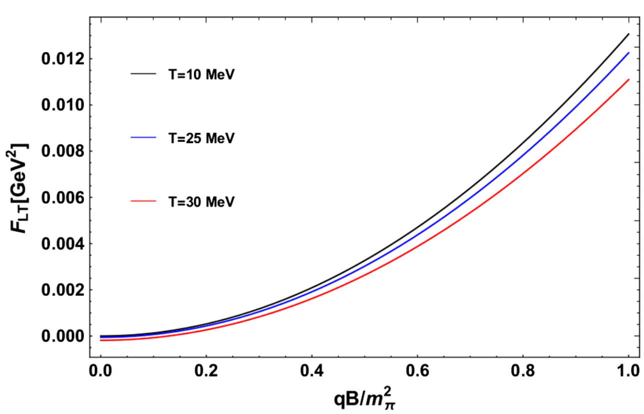

FIG. 4. F_{LT} vs T.

VII. CONCLUSIONS

Using the imaginary time formalism for dealing with temperature effects and the Schwinger propagator for handling the external magnetic field, we have analyzed the influence of temperature and a weak external magnetic field on the renormalon diagram in the theory $\lambda\phi^4$.

Initially we considered only temperature effects, finding the same results obtained in the frame of thermofield dynamics [43]. This again confirms the validity of both formalisms.

In the case of the thermomagnetic corrections to our renormalon type of diagram, we obtained a nonanalytic closed expression. However, for the low- and high-temperature regions it is possible to have analytic expressions. The agreement between our analytic expression in the high-temperature regions and the numerical results is amazing, being valid for a wide temperature region. Something interesting is the competition we found, in the calculation of the residue, between the magnetic field and temperature. As we said, in the low-temperature region and for low magnetic field strength, the residue grows. As soon as the temperature starts to increase, this growing behavior becomes less pronounced. We also found in the high-temperature region that, for example, for $T = 60$ MeV we still have a growing behavior but with much less concavity. In the case of really high temperature, the residue diminishes with the magnetic field. It is interesting to point out that this scenario was also found in the behavior of the $\pi - \pi$ scattering lengths [45,46] where we have exactly the same competition between temperature and magnetic field strength.

ACKNOWLEDGMENTS

M. L. and R. Z. acknowledge support from Agencia Nacional de Investigación y Desarrollo (ANID) ANID/CONICYT FONDECYT Regular (Chile) under Grant No. 1200483. M. L., L. M. and R. Z. acknowledge support from Fondecyt under Grant No. 1170107. M. L. and R. Z. acknowledge also support from Fondecyt under Grant No. 1190192. M. L. also acknowledges support from Anid/Pia/Basal (Chile) under Grant No. FB082.

APPENDIX: LOW- AND HIGH-TEMPERATURE APPROXIMATIONS FOR THE FUNCTION $h(\beta)$

In this appendix we analyze the function $h(\beta)$. As this function is nonanalytic, we are going to study its behavior for the high- and low-temperature cases separately.

We will start with the high-temperature case $h_{HT}(\beta)$. We have

$$h(\beta) = \int_0^\infty \frac{k^2 dk}{\sqrt{k^2+m^2}} \frac{1}{e^{\sqrt{k^2+m^2}/T} - 1}. \tag{A1}$$

Defining $m/T = y$ and $k/T = x$, we get

$$h(\beta) = T^2 \int_0^\infty \frac{dx\, x^2}{\sqrt{x^2+y^2}} \frac{1}{e^{\sqrt{x^2+y^2}} - 1}. \tag{A2}$$

The last expression can be related to the functions presented in the Appendix of Ref. [40]. We have $h(\beta) = T^2\Gamma(3)h_3(y) = 2T^2 h_3(y)$. To find $h_3(y)$, we use the relation

$$\frac{dh_3(y)}{dy} = \frac{-y h_1(y)}{2}, \tag{A3}$$

where

$$h_1^{HT}(y) = \frac{\pi}{2y} + \frac{1}{2}\log\left(\frac{y}{4\pi}\right) + \frac{1}{2}\gamma_E - \frac{1}{4}\zeta(3)\left(\frac{y}{2\pi}\right)^2 + \frac{3}{16}\zeta(5)\left(\frac{y}{2\pi}\right)^4 + \cdots. \tag{A4}$$

Therefore, we obtain

$$\frac{dh_3^{HT}(y)}{dy} = -\frac{\pi}{4} - \frac{y}{4}\log\left(\frac{y}{4\pi}\right) - \frac{y}{4}\gamma_E + \frac{y}{8}\zeta(3)\left(\frac{y}{2\pi}\right)^2 - \frac{3y}{32}\zeta(5)\left(\frac{y}{2\pi}\right)^4 + \cdots. \tag{A5}$$

Solving the previous equation,

$$h_3^{HT}(y) = -\frac{\pi y}{4} + \frac{y^2}{8}\left[\frac{1}{2} + \log\left(\frac{4\pi}{y}\right) - \gamma\right] + \frac{y^4}{128\pi^2}\zeta(3) - \frac{y^6}{1024\pi^2}\zeta(5) + C_1 + \cdots. \tag{A6}$$

In order to find the constant of integration (C_1), we calculate

$$h_3(0) = \frac{1}{\Gamma(3)}\int_0^\infty dx \frac{x^2}{x}\frac{1}{e^x - 1} = \frac{1}{\Gamma(3)}\frac{\pi^2}{6} = \frac{\pi^2}{12} \tag{A7}$$

$$\Rightarrow C_1 = \frac{\pi^2}{12}. \tag{A8}$$

Therefore,

$$h_3^{HT}(y) = \frac{\pi^2}{12} - \frac{\pi y}{4} + \frac{y^2}{8}\left[\frac{1}{2} + \log\left(\frac{4\pi}{y}\right) - \gamma\right] + \frac{y^4}{128\pi^2}\zeta(3) - \frac{y^6}{1024\pi^2}\zeta(5) + \cdots. \tag{A9}$$

Finally, for the high-temperature case we obtain

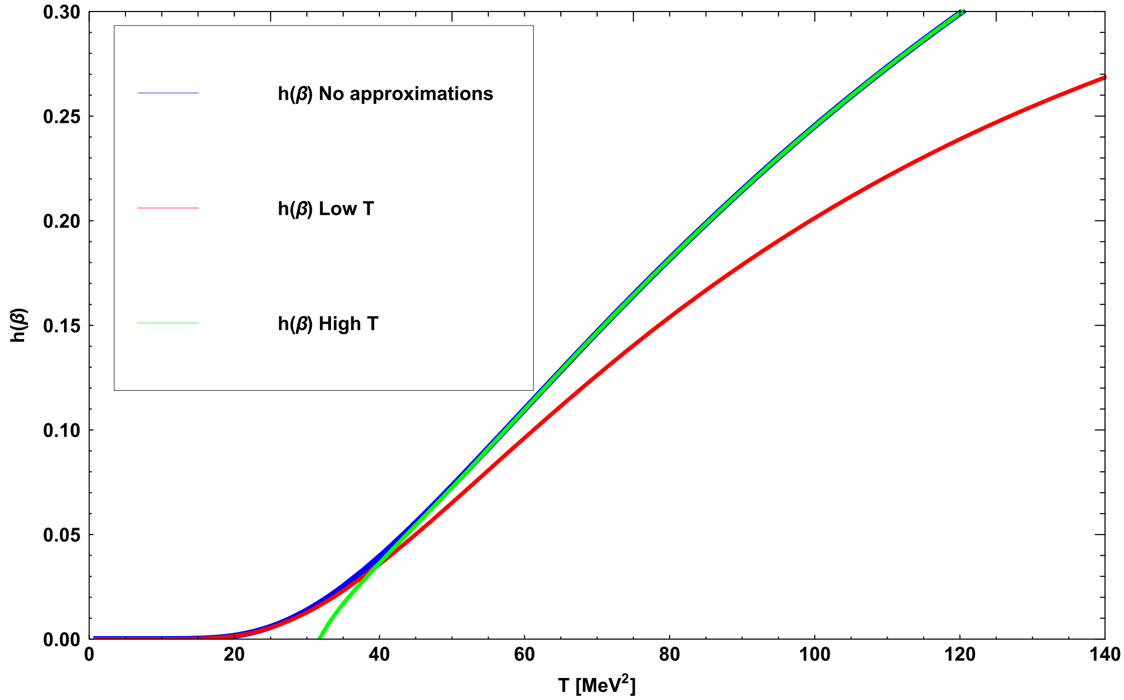

FIG. 5. Comparison of the function $h(\beta)$ with the high- and low-temperature approximations. The blue line corresponds to the numerical evaluation of $h(\beta)$, the red line to the case of $h(\beta)$ at low temperature, and the green line to the case of $h(\beta)$ at high temperature.

$$\begin{aligned} h_{HT}(\beta) &= 2T^2 h_3^{HT}(y) = 2T^2 h_3^{HT}\left(\frac{m}{T}\right) \\ &= 2T^2\left(\frac{\pi^2}{12} - \frac{\pi m}{4T} + \frac{m^2}{8T^2}\left[\frac{1}{2} + \log\left(\frac{4\pi T}{m}\right) - \gamma\right]\right. \\ &\quad \left. + \frac{m^4}{128\pi^2 T^4}\zeta(3) - \frac{m^6}{1024\pi^4 T^6}\zeta(5) + \cdots\right). \end{aligned} \tag{A10}$$

Now we will analyze the behavior of $h(\beta)$ in the low-temperature regime. We have

$$h(\beta) = \int_0^\infty \frac{k^2\, dk}{\sqrt{k^2+m^2}} \frac{1}{e^{\sqrt{k^2+m^2}/T} - 1}. \tag{A11}$$

Using $\omega^2 = k^2 + m^2$, we get

$$h(\beta) = \int_0^\infty \frac{(\omega^2 - m^2)\omega\, d\omega}{\omega\sqrt{\omega^2 - m^2}} \frac{1}{e^{\omega/T} - 1}, \tag{A12}$$

which can be written as

$$h(\beta) = \int_m^\infty d\omega \sqrt{\omega^2 - m^2} \frac{e^{-\omega/T}}{1 - e^{-\omega/T}}. \tag{A13}$$

In the case of low temperature, the last part of the previous equation corresponds to a geometric series. Therefore,

$$h_{LT}(\beta) = \sum_{n=1}^\infty \int_m^\infty d\omega \sqrt{\omega^2 - m^2} e^{-n\omega/T}. \tag{A14}$$

Performing the integral, we get

$$h_{LT}(\beta) = \sum_{n=1}^\infty \frac{mT}{n} K_1\left(\frac{mn}{T}\right). \tag{A15}$$

Note that for low temperature

$$\frac{mT}{n} K_1\left(\frac{mn}{T}\right) \overrightarrow{[T \to 0]} \left(\frac{T^3 m\pi}{2n^3}\right)^{1/2} e^{-mn/T}. \tag{A16}$$

Using the above result, we have

$$h_{LT}(\beta) = \sum_{n=1}^\infty \left(\frac{T^3 m\pi}{2n^3}\right)^{1/2} e^{-mn/T}. \tag{A17}$$

The above sum is analytical, and corresponds to the polylogarithm functions (Li). Finally, we obtain

$$h_{LT}(\beta) = \left(\frac{T^3 m\pi}{2}\right)^{1/2} \mathrm{Li}_{3/2}(e^{-m/T}). \tag{A18}$$

Now we are going to plot the function $h(\beta)$, comparing its numerical value with the high- and low-temperature approximations as it is shown in Fig. 5. We note that our approximation for the low-temperature case, up to a value of around $T \sim 40$ MeV, is quite good, whereas for a temperature greater than $T \sim 40$ MeV the high-temperature approximation is also excellent. Therefore, with our approximations, we are able to cover in an analytic way the whole range of temperatures. It is important, however, to stress how sensible our analytic expressions are. For example, if we do not include the terms that involve the Riemann zeta factors in the high-temperature region, the approximation turns out to be valid only for a temperature greater than $T \sim 140$ MeV.

[1] F. J. Dyson, Phys. Rev. **85**, 631 (1952).
[2] G. Altarelli, Introduction to renormalons, Report No. CERN-TH/95-309, 1995.
[3] V. Rivasseau, *From Perturbative to Constructive Renormalization* (Princeton University Press, Princeton, NJ, 1991).
[4] F. C. Khanna, A. P. C. Malbouisson, J. M. C. Malbouisson, and A. R. Santana, *Thermal Quantum Field Theory: Algebraic Aspects and Applications* (World Scientific, Singapore, 2009).
[5] M. Beneke, Phys. Rep. **317**, 1 (1999).
[6] A. Maiezza and J. C. Vasquez, Ann. Phys. (Amsterdam) **394**, 84 (2018).
[7] E. Cavalcanti, J. A Lourenço, C. A. Linhares, and A. P. C. Malbouisson, Phys. Rev. D **98**, 045013 (2018).
[8] D. J. Gross, R. D. Pisarski, and L. G. Yaffe, Rev. Mod. Phys. **53**, 43 (1981).
[9] T. Shäfer and E. V. Shuryak, Rev. Mod. Phys. **70**, 323 (1998).
[10] D. E. Kharzeev, L. D. McLerran, and H. J. Warringa, Nucl. Phys. **A803**, 227 (2008).
[11] G. S. Bali, B. B. Brandt, G. Endrődi, and B. Glässle, Phys. Rev. Lett. **121**, 072001 (2018).
[12] S. Fayazbakhsh and N. Sadooghi, Phys. Rev. D **88**, 065030 (2013).
[13] A. Ayala, J. L. Hernández, L. A. Hernández, R. L. S Farias, and R. Zamora, Phys. Rev. D **103**, 054038 (2021).
[14] A. Ayala, J. L. Hernández, L. A. Hernández, R. L. S Farias, and R. Zamora, Phys. Rev. D **102**, 114038 (2020).
[15] C. A. Dominguez, L. A. Hernández, M. Loewe, C. Villavicencio, and R. Zamora, Phys. Rev. D **102**, 094007 (2020).
[16] Yu. A. Simonov, Phys. At. Nucl. **79**, 455 (2016).
[17] R. M. Aguirre, Eur. Phys. J. A **55**, 28 (2019).
[18] T. Yoshida and K. Suzuki, Phys. Rev. D **94**, 074043 (2016).
[19] D. Dudal and T. G. Mertens, Phys. Rev. D **91**, 086002 (2015).
[20] K. Marasinghe and K. Tuchin, Phys. Rev. C **84**, 044908 (2011).
[21] P. Gubler, K. Hattori, S. H. Lee, M. Oka, S. Ozaki, and K. Suzuki, Phys. Rev. D **93**, 054026 (2016).
[22] C. S. Machado, S. I. Finazzo, R. D. Matheus, and J. Noronha, Phys. Rev. D **89**, 074027 (2014).
[23] S. Cho, K. Hattori, S. H. Lee, K. Morita, and S. Ozaki, Phys. Rev. Lett. **113**, 172301 (2014).
[24] A. Ayala, M. Loewe, and R. Zamora, Phys. Rev. D **91**, 016002 (2015).
[25] A. Ayala, R. L. S. Farias, S. Hernández-Ortíz, L. A. Hernández, D. M. Paret, and R. Zamora, Phys. Rev. D **98**, 114008 (2018).
[26] S. Cho, K. Hattori, S. H. Lee, K. Morita, and S. Ozaki, Phys. Rev. D **91**, 045025 (2015).
[27] S. Ghosh, A. Mukherjee, M. Mandal, S. Sarkar, and P. Roy, Phys. Rev. D **94**, 094043 (2016).
[28] A. Bandyopadhyay and S. Mallik, Eur. Phys. J. C **77**, 771 (2017).
[29] S. S. Avancini, W. R. Tavares, and M. B. Pinto, Phys. Rev. D **93**, 014010 (2016).
[30] S. S. Avancini, R. L. Farias, M. B. Pinto, W. R. Tavares, and V. S. Timteo, Phys. Lett. B **767**, 247 (2017).
[31] A. Ayala, C. A. Dominguez, L. A. Hernández, M. Loewe, and R. Zamora, Phys. Rev. D **92**, 096011 (2015).
[32] A. Ayala, M. Loewe, A. J. Mizher, and R. Zamora, Phys. Rev. D **90**, 036001 (2014).
[33] A. Ayala, S. Hernandez-Ortiz, L. A. Hernandez, V. Knapp-Perez, and R. Zamora, Phys. Rev. D **101**, 074023 (2020).
[34] E. Cavalcanti, Phys. Rev. D **103**, 025019 (2021).
[35] N. A. Dondi, G. V. Dunne, M. Reichart, and F. Sannino, Phys. Rev. D **102**, 035005 (2020).
[36] J. S. Schwinger, Phys. Rev. **82**, 664 (1951).
[37] A. Ayala, A. Sanchez, G. Piccinelli, and S. Sahu, Phys. Rev. D **71**, 023004 (2005).
[38] A. Ayala, J. Castaño-Yepes, L. A. Hernández, J. Salinas, and R. Zamora, Eur. Phys. J. A **57**, 140 (2021).
[39] M. Le Bellac, *Thermal Field Theory* (Cambridge University Press, Cambridge, England, 1996).
[40] J. I. Kapusta and C. Gale, *Finite-Temperature Field Theory Principles and Applications* (Cambridge University Press, Cambridge, England, 2006).
[41] G. H. Hardy, *Divergent Series* (Oxford University Press, New York, 1949).
[42] D. Bailin and A. Love, *Introduction to Gauge Field Theory* (Institute of Physics Publishing, Bristol and Philadelphia, 1993).
[43] M. Loewe and C. Valenzuela, Mod. Phys. Lett. A **15**, 1181 (2000).
[44] M. Correa, M. Loewe, D. Valenzuela, and R. Zamora, Phys. Rev. D **99**, 096024 (2019).
[45] M. Loewe, L. Monje, and R. Zamora, Phys. Rev. D **97**, 056023 (2018).
[46] M. Loewe, L. Monje, E. Muñoz, A. Raya, and R. Zamora, Phys. Rev. D **99**, 056002 (2019).